

# Increased bisecting and core-fucosylated *N*-glycans on mutant human amyloid precursor proteins

Keiko Akasaka-Manyá · Hiroshi Manyá ·  
Yoko Sakurai · Boguslaw S. Wojczyk ·  
Steven L. Spitalnik · Tamao Endo

Received: 18 February 2008 / Revised: 21 April 2008 / Accepted: 23 April 2008 / Published online: 3 June 2008  
© Springer Science + Business Media, LLC 2008

**Abstract** Alteration of glycoprotein glycans often changes various properties of the glycoprotein. To understand the significance of *N*-glycosylation in the pathogenesis of early-onset familial Alzheimer's disease (AD) and in  $\beta$ -amyloid ( $A\beta$ ) production, we examined whether the mutations in the *amyloid precursor protein* (APP) gene found in familial AD affect the *N*-glycans on APP. We purified the secreted forms of wild-type and mutant human APPs (both the Swedish type and the London type) produced by transfected C17 cells and determined the *N*-glycan structures of these three recombinant APPs. Although the major *N*-glycan species of the three APPs were similar, both mutant APPs contained higher contents of bisecting *N*-acetylglucosamine and core-fucose residues as compared to wild-type APP. These results demonstrate that familial AD mutations in the polypeptide backbone of APP can affect processing of the attached *N*-glycans; however, whether these changes in *N*-glycosylation affect  $A\beta$  production remains to be established.

**Keywords** Amyloid precursor protein · *N*-glycan · Alzheimer's disease · Bisecting *N*-acetylglucosamine · Core-fucose

## Abbreviations

AB	aminobezamide
$A\beta$	$\beta$ -amyloid
AD	Alzheimer's disease
APP	amyloid precursor protein
FUT8	$\alpha$ 1–6 fucosyltransferase
GnT-III	<i>N</i> -acetylglucosaminyltransferase III
HPLC	high-performance liquid chromatography
GU	glucose unit

## Introduction

Alzheimer's disease (AD) is a neurodegenerative disorder characterized pathologically by extracellular senile plaques and intraneuronal neurofibrillary tangles.  $\beta$ -amyloid ( $A\beta$ ), the major component of senile plaques, is a fragment of a large membrane-spanning glycoprotein, amyloid precursor protein (APP), and is generated by cleavage of APP by  $\beta$ - and  $\gamma$ -secretases. According to the "amyloid cascade hypothesis", the abnormal accumulation of  $A\beta$  leads to subsequent neurodegenerative processes, finally resulting in neuronal death. Because  $A\beta$  is also produced in normal brain, the excess of  $A\beta$  production, and/or the reduction of  $A\beta$  degradation, are presumed to occur in the brains of AD patients. Two major types of  $A\beta$  are produced depending on the cleavage site of  $\gamma$ -secretase:  $A\beta$ 40 and  $A\beta$ 42;  $A\beta$ 42 has a greater tendency to produce insoluble deposits and is a major component of the amyloid plaques found in brain.

Many studies have addressed the pathogenesis of AD. Several relevant genes were identified by studying pedi-

---

Keiko Akasaka-Manyá and Hiroshi Manyá contributed equally to this work.

---

K. Akasaka-Manyá · H. Manyá · Y. Sakurai · T. Endo (✉)  
Glycobiology Research Group,  
Tokyo Metropolitan Institute of Gerontology,  
Foundation for Research on Aging and Promotion  
of Human Welfare,  
35-2 Sakaecho, Itabashi-ku,  
Tokyo 173-0015, Japan  
e-mail: endo@tmig.or.jp

B. S. Wojczyk · S. L. Spitalnik  
Department of Pathology and Cell Biology,  
Columbia University Medical Center,  
New York, NY 10032, USA

genes of familial AD. Most of the mutations in these genes up-regulate A $\beta$  production. For example, missense mutations adjacent to the  $\beta$ - and  $\gamma$ -secretase cleavage sites in APP, and mutations in presenilin 1 and 2, the main molecules of the  $\gamma$ -secretase complex, augment A $\beta$ 42 production and lead to autosomal-dominant, early-onset forms of familial AD [1, 2].

In contrast to familial AD, little is known about the causes of sporadic AD, although over 90% of AD patients have the sporadic form. In the brains of these patients, a decrease in A $\beta$  degradation is assumed to cause A $\beta$  accumulation because there is no evidence for excess A $\beta$  production. The current study focuses on the role of *N*-glycans in the biology of APP. Alterations of the structures and/or amounts of glycans on various glycoproteins can occur during aging and diseases. For example, neural cell adhesion molecule (NCAM) has polysialic acids in the fetal and neonatal periods, although polysialylated NCAM is predominantly not expressed in adults [3–5]. As another example, the  $\alpha$ 1-6-fucosylated form of  $\alpha$ -fetoprotein (AFP-L3) is a tumor marker for hepatocellular carcinoma. Thus, *N*-glycosylated  $\alpha$ -fetoprotein, which is produced in the liver, is found in serum and serum levels increase in patients with hepatocellular carcinoma, chronic hepatitis, and liver cirrhosis. However, AFP-L3 is only found in the serum of patients with hepatocellular carcinoma [6, 7]. As a final example, glycoproteins from non-malignant cells preferentially express the disialyl Lewis<sup>a</sup> structure, but malignant transformation significantly decreases disialyl Lewis<sup>a</sup> levels and increases production of sialyl Lewis<sup>a</sup> [8].

Glycoprotein glycans not only affect protein stability and conformation, but also influence cellular localization and trafficking [9]. APP undergoes several posttranslational modifications, including *N*- and *O*-linked glycosylation [10–12]. Previous studies showed that *N*-glycosylation and the resulting *N*-glycan structures modulated APP processing [13–15]. We previously characterized the *N*-glycan structures of human APP produced by transfected Chinese hamster ovary cells. To understand the significance of *N*-glycans in the pathogenic mechanisms of early-onset familial AD, we currently examined whether familial AD mutations in the human *APP* gene, which are known to increase A $\beta$  production, also lead to alterations in *N*-glycan structure. To this end, we studied Swedish type (Lys595/Met596 to Asn/Leu) and London type (Val642 to Phe) mutant APP. The Swedish type mutation is known to increase the amount of A $\beta$ 42 secretion six to seven times [16] and the London type mutation doubles the ratio of secreted A $\beta$ 42 to secreted A $\beta$ 40 [1, 2, 17]. To clarify the effects of these mutations on APP *N*-glycan structures, we transfected the cDNAs for wild-type APP695 and these two mutations [Val642 to Phe (*i.e.*,  $\Delta$ F) and Lys595/Met596 to Asn/Leu (*i.e.*,  $\Delta$ NL)] into mouse C17 neuroblastoma. We

found significant structural differences in the *N*-glycans when comparing wild-type and mutant APPs.

## Experimental procedures

**Enzymes** *Arthrobacter ureafaciens* sialidase was purchased from Nacalai Tesque (Kyoto, Japan), and Sigma-Aldrich Co. (St. Louis, MO, USA). *Streptococcus pneumoniae*  $\beta$ -galactosidase,  $\beta$ -*N*-acetylhexosaminidase, and beef kidney  $\alpha$ -fucosidase were purchased from Roche Diagnostics (Basel, Switzerland). Jack bean  $\beta$ -*N*-acetylhexosaminidase and  $\alpha$ -mannosidase were purchased from Seikagaku Co. (Tokyo, Japan). *Streptococcus 6646K*  $\beta$ -galactosidase and green coffee bean  $\alpha$ -galactosidase were purchased from Toyobo Co. Ltd. (Osaka, Japan). *Clostridium perfringens* endo- $\beta$ -galactosidase C was provided by Dr. Takashi Muramatsu [18].

**Preparation of APP** The secreted form of recombinant human APP was purified from the conditioned medium produced by mouse neuroblastoma C17 cells that had been stably transfected with the full-length, wild-type 695 amino acid form of human APP, or with either the  $\Delta$ F or  $\Delta$ NL mutant, as described previously [12]. Following DEAE-sepharose chromatography, immunoaffinity chromatography, and FPLC using a Mono Q HR5/5 column, the isolated proteins were analyzed by SDS-PAGE (10% gel), visualized with Gradipure gel electrophoresis stain (VWR, West Chester, PA, USA), and identified by Western blotting with goat anti-APP antiserum.

**Release of *N*-glycans from APP** The purified, secreted form of wild-type or mutant APP (500  $\mu$ g) was thoroughly dried over P<sub>2</sub>O<sub>5</sub> in vacuo and subjected to hydrazinolysis at 100° C for 10 h. The liberated *N*-glycans were *N*-acetylated and purified, as described previously [19]. This procedure quantitatively releases the *N*-glycans of glycoproteins as oligosaccharides. Following *N*-acetylation, the samples were separated by paper chromatography using 1-butanol/ethanol/water (4:1:1, *v/v*) for 18 h. To isolate the *N*-glycans, the area of the paper from the origin to the migration position of authentic lactose was extracted with water.

**2-Aminobenzamide (2AB) Derivatization of *N*-glycans** The total *N*-glycans obtained above were labeled with 2-aminobenzamide (2AB), as described previously [19]. To detect the 2AB-labeled *N*-glycans, fluorescence emission was monitored at 420 nm with excitation at 330 nm.

**Oligosaccharides** The following 2AB-labeled oligosaccharide standards were purchased from ProZyme (San Leandro, CA, USA): NA2, Gal $\beta$ 1-4GlcNAc $\beta$ 1-2Man $\alpha$ 1-6(Gal $\beta$ 1-

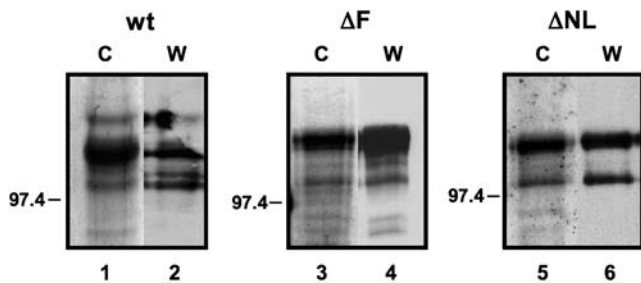


**Fig. 1** SDS-PAGE analysis of purified APPs. The secreted forms of recombinant human APPs were purified from the conditioned medium of transfected C17 cells. Following DEAE-sepharose chromatography, immunoaffinity chromatography, and FPLC using a Mono Q HR5/5 column, the isolated proteins were analyzed by SDS-PAGE (10% gel) and detected with Gradipure gel electrophoresis stain (lanes C) or identified by Western blotting (lanes W). The same purification procedure was applied to purify wild type protein (lanes 1 and 2), the  $\Delta F$  mutant (lanes 3 and 4), and the  $\Delta NL$  mutant (lanes 5 and 6). The migration position of the phosphorylase B molecular weight standard (97.4 kDa) is indicated on the left of each panel

4GlcNAc $\beta$ 1-2Man $\alpha$ 1-3)Man $\beta$ 1-4GlcNAc $\beta$ 1-4GlcNAc-2AB (Gal<sub>2</sub>·GlcNAc<sub>2</sub>·Man<sub>3</sub>·GlcNAc·GlcNAc-2AB); NA2F, Gal $\beta$ 1-4GlcNAc $\beta$ 1-2Man $\alpha$ 1-6(Gal $\beta$ 1-4GlcNAc $\beta$ 1-2Man $\alpha$ 1-3)Man $\beta$ 1-4GlcNAc $\beta$ 1-4(Fuc $\alpha$ 1-6)GlcNAc-2AB (Gal<sub>2</sub>·GlcNAc<sub>2</sub>·Man<sub>3</sub>·GlcNAc·Fuc·GlcNAc-2AB); NA2FB, Gal $\beta$ 1-4GlcNAc $\beta$ 1-2Man $\alpha$ 1-6(Gal $\beta$ 1-4GlcNAc $\beta$ 1-2Man $\alpha$ 1-3)(GlcNAc $\beta$ 1-4)Man $\beta$ 1-4GlcNAc $\beta$ 1-4(Fuc $\alpha$ 1-6)GlcNAc-2AB (Gal<sub>2</sub>·GlcNAc<sub>2</sub>·Man<sub>2</sub>·GlcNAc·Man·GlcNAc·Fuc·GlcNAc-2AB); NA3, Gal $\beta$ 1-4GlcNAc $\beta$ 1-2Man $\alpha$ 1-6[Gal $\beta$ 1-4GlcNAc $\beta$ 1-2(Gal $\beta$ 1-4GlcNAc $\beta$ 1-4)Man $\alpha$ 1-3]Man $\beta$ 1-4GlcNAc $\beta$ 1-4GlcNAc-2AB (Gal<sub>3</sub>·GlcNAc<sub>3</sub>·Man<sub>3</sub>·GlcNAc·GlcNAc-2AB); M5, Man $\alpha$ 1-6(Man $\alpha$ 1-3)Man $\alpha$ 1-6(Man $\alpha$ 1-3)Man $\beta$ 1-4GlcNAc $\beta$ 1-4GlcNAc-2AB (Man<sub>5</sub>·GlcNAc·GlcNAc-2AB); NGA2, GlcNAc $\beta$ 1-2Man $\alpha$ 1-6(GlcNAc $\beta$ 1-2Man $\alpha$ 1-3)Man $\beta$ 1-4GlcNAc $\beta$ 1-4GlcNAc-2AB (GlcNAc<sub>2</sub>·Man<sub>3</sub>·GlcNAc·GlcNAc-2AB); NGA2F, GlcNAc $\beta$ 1-2Man $\alpha$ 1-6(GlcNAc $\beta$ 1-2Man $\alpha$ 1-3)Man $\beta$ 1-4GlcNAc $\beta$ 1-4(Fuc $\alpha$ 1-6)GlcNAc-2AB (GlcNAc<sub>2</sub>·Man<sub>3</sub>·GlcNAc·Fuc·GlcNAc-2AB); NGA2FB, GlcNAc $\beta$ 1-2Man $\alpha$ 1-6(GlcNAc $\beta$ 1-2Man $\alpha$ 1-3)(GlcNAc $\beta$ 1-4)Man $\beta$ 1-4GlcNAc $\beta$ 1-4(Fuc $\alpha$ 1-6)GlcNAc-2AB (GlcNAc<sub>2</sub>·Man<sub>2</sub>·GlcNAc·Man·GlcNAc·Fuc·GlcNAc-2AB); NGA3, GlcNAc $\beta$ 1-2Man $\alpha$ 1-6[GlcNAc $\beta$ 1-2(GlcNAc $\beta$ 1-4)Man $\alpha$ 1-3]Man $\beta$ 1-4GlcNAc $\beta$ 1-4GlcNAc-2AB (GlcNAc<sub>3</sub>·Man<sub>3</sub>·GlcNAc·GlcNAc-2AB). M3, Man $\alpha$ 1-6(Man $\alpha$ 1-3)Man $\beta$ 1-4GlcNAc $\beta$ 1-4GlcNAc-2AB (Man<sub>3</sub>·GlcNAc·GlcNAc-2AB) was obtained by digestion of NA2 with a mixture of streptococcal  $\beta$ -galactosidase and  $\beta$ -*N*-acetylhexosaminidase. M1, Man $\beta$ 1-4GlcNAc $\beta$ 1-4GlcNAc-2AB (Man·GlcNAc·GlcNAc-2AB) was obtained by digestion of M3 with jack bean  $\alpha$ -mannosidase.

**Analytical Methods** Anion-exchange chromatography of 2AB-labeled *N*-glycans was carried out on a high-performance liquid chromatography (HPLC) apparatus equipped with a Mono Q HR5/5 column. Elution was performed with water for 10 min, then with a linear gradient from 0 to 600 mM ammonium acetate (pH 4.0) over 35 min at a flow rate of 1 ml/min at room temperature.

Normal-phase HPLC was carried out on a GlycoSep N column (ProZyme) by elution with a 250 mM ammonium acetate-acetonitrile gradient solvent system at a flow rate 1 ml/min at 30°C. The 250 mM acetate/acetonitrile ratio was changed linearly from 20:80 to 53:47 (v/v) over 132 min. The column was calibrated using a mixture of 2AB-labeled glucose oligomers, the elution positions of which were used to obtain the glucose unit (GU) values for each glycan.

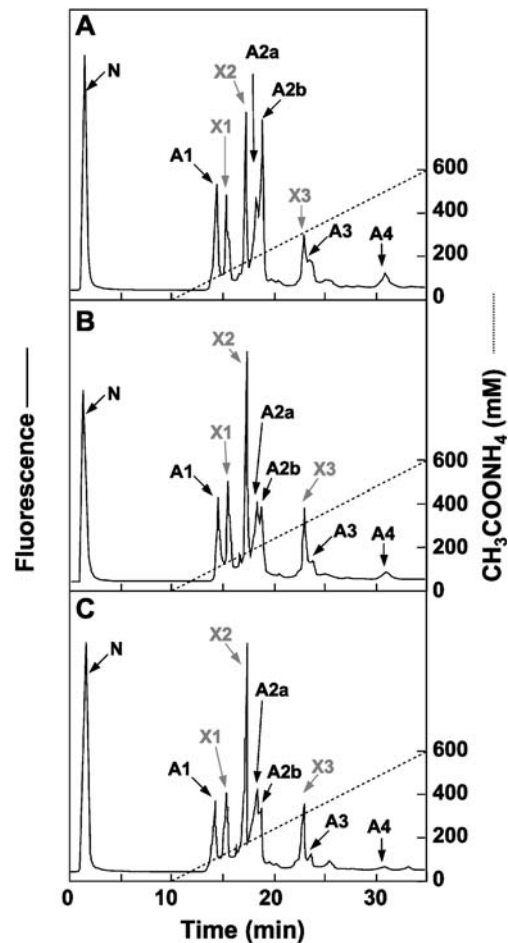


**Fig. 2** Anion-exchange chromatography of the 2AB-labeled *N*-glycans isolated from purified recombinant APPs. The 2AB-labeled *N*-glycans were subjected to HPLC using a Mono Q HR5/5 column, as described in “Experimental procedures.” a–c *N*-glycans from wild type APP695,  $\Delta F$  mutant, and  $\Delta NL$  mutant, respectively

**Table 1** Fractionation of acidic *N*-glycans from three APPs

Peak	Molar ratio (%)		
	wt	$\Delta F$	$\Delta NL$
A1	25.7	37.2	33.5
A2a	12.5	20.7	25.5
A2b	43.3	29.9	32.0
A3	12.0	9.0	5.3
A4	6.5	3.2	3.7

Reversed-phase HPLC was carried out on a Cosmosil 5C<sub>18</sub>-AR column (Nacalai Tesque), which was equilibrated with 100 mM ammonium acetate buffer, pH 4.0, and eluted with a gradient of 1-butanol (0.25–1% butanol) over 120 min at a flow rate of 1 ml/min at 55°C.

**Glycosidase Digestion** *N*-Glycans were incubated with one of the following mixtures for 18 h at 37°C: (1) *A. ureafaciens* sialidase (25 mU) in 30  $\mu$ l of 500 mM ammonium acetate buffer, pH 5.0; (2) Streptococcal 6646K  $\beta$ -galactosidase (2 mU) in 50  $\mu$ l of 100 mM citrate phosphate buffer, pH 6.0; (3) Streptococcal  $\beta$ -galactosidase (12.5 mU) in 50  $\mu$ l of 300 mM citrate phosphate buffer, pH 6.0; (4) Streptococcal  $\beta$ -*N*-acetylhexosaminidase (5 mU) in 50  $\mu$ l of 300 mM citrate phosphate buffer, pH 6.0; (5) jack bean  $\beta$ -*N*-acetylhexosaminidase (0.5 U) in 40  $\mu$ l of 300 mM citrate phosphate buffer, pH 5.0; (6)  $\alpha$ -mannosidase (1 U) in 50  $\mu$ l of 50 mM sodium acetate buffer, pH 4.5; (7)  $\beta$ -mannosidase (10 mU) in 50  $\mu$ l of 50 mM citrate phosphate buffer, pH 4.0; (8)  $\alpha$ -fucosidase (10 mU) in 40  $\mu$ l of 200 mM citrate phosphate buffer, pH 6.0. One drop of toluene was added to all reaction mixtures to inhibit bacterial growth during incubation. Heating the reaction mixture in a boiling water bath for 3 min terminated the digestions. The digested samples were then desalted by HPLC using the Cosmosil 5C<sub>18</sub>-AR column, using the approach described above for the neutralized 2AB-labeled *N*-glycans; the remaining ammonium acetate was removed by extensive evaporation.

## Results

**SDS-PAGE of the Secreted Form of Purified Human APP** The secreted form of recombinant human APP was purified from the conditioned medium of C17 cells that had been stably transfected with the full-length, 695 amino acid form of wild-type human APP. Following DEAE-Sepharose chromatography, immunoaffinity chromatography, and Mono Q column chromatography, the isolated proteins were analyzed by SDS-PAGE (10% gel) and detected with

Gradipure gel electrophoresis stain (Fig. 1, lanes C) or identified by Western blotting with anti-APP antibody (Fig. 1, lanes W). The same purification procedure was applied to purify the wild-type protein (Fig. 1, lanes 1 and 2), the  $\Delta F$  mutant (Fig. 1, lanes 3 and 4), and the  $\Delta NL$  mutant (Fig. 1, lanes 5 and 6).

**Fractionation of Liberated *N*-glycans by Anion-exchange Chromatography** The 2AB-labeled *N*-glycan mixtures obtained from purified APP by hydrazinolysis were separated into neutral (N) and acidic (A1, A2a, A2b, A3, and A4) fractions by anion-exchange chromatography on a Mono Q HR5/5 column (Fig. 2). The percentage molar ratios of the *N*-glycans in the acidic fractions, calculated on the basis of their fluorescence intensity, are shown in Table 1.

By exhaustive digestion with *A. ureafaciens* sialidase, all acidic fractions (*i.e.* A1, A2a, A2b, A3, and A4) were completely converted into neutral *N*-glycans, indicating that the only acidic residues in these *N*-glycans are sialic acids. The neutral *N*-glycan fractions from A1, A2a, A2b, A3, and A4 were named A1N, A2aN, A2bN, A3N, and A4N, respectively.

The X1, X2, and X3 fractions seen in Fig. 2 were not derived from *N*-glycans, because these fractions were detected in the region of 1–2 GU in normal phase column chromatography after sialidase digestion (data not shown). Therefore, these peaks most likely represent derivatives of *O*-glycans. For this reason, we did not perform any further structural studies of these fractions.

**Structural Study of the *N*-glycans found in the Acidic Fractions** The sialidase-digested *N*-glycans from each acidic fraction were subjected to normal phase column chromatography (Fig. 3). Each component (a–r) in Fig. 3 was fractionated as a single peak by reversed-phase column chromatography (Fig. 4). Several components (c and d; f, g, h and i; m and n) in A1N and A2aN fractions were eluted as a mixture on normal phase column, but these were separated as a single component by reversed-phase column chromatography. Remaining components (a, b, e, k, o and p) in A1N and A2aN fractions were eluted as a single peak on both normal and reversed-phase columns (Figs. 3 and 4). The components p, q and r in A2bN, A3N and A4N in Fig. 3 were eluted as a single peak on the reversed-phase column (data not shown).

To determine the structures of each component, they were then subjected to sequential exoglycosidase digestion and analyzed by HPLC as shown in Fig. 5. When component “a” was incubated with streptococcal  $\beta$ -galactosidase, which only cleaves the Gal $\beta$ 1–4GlcNAc linkage [20], it eluted at

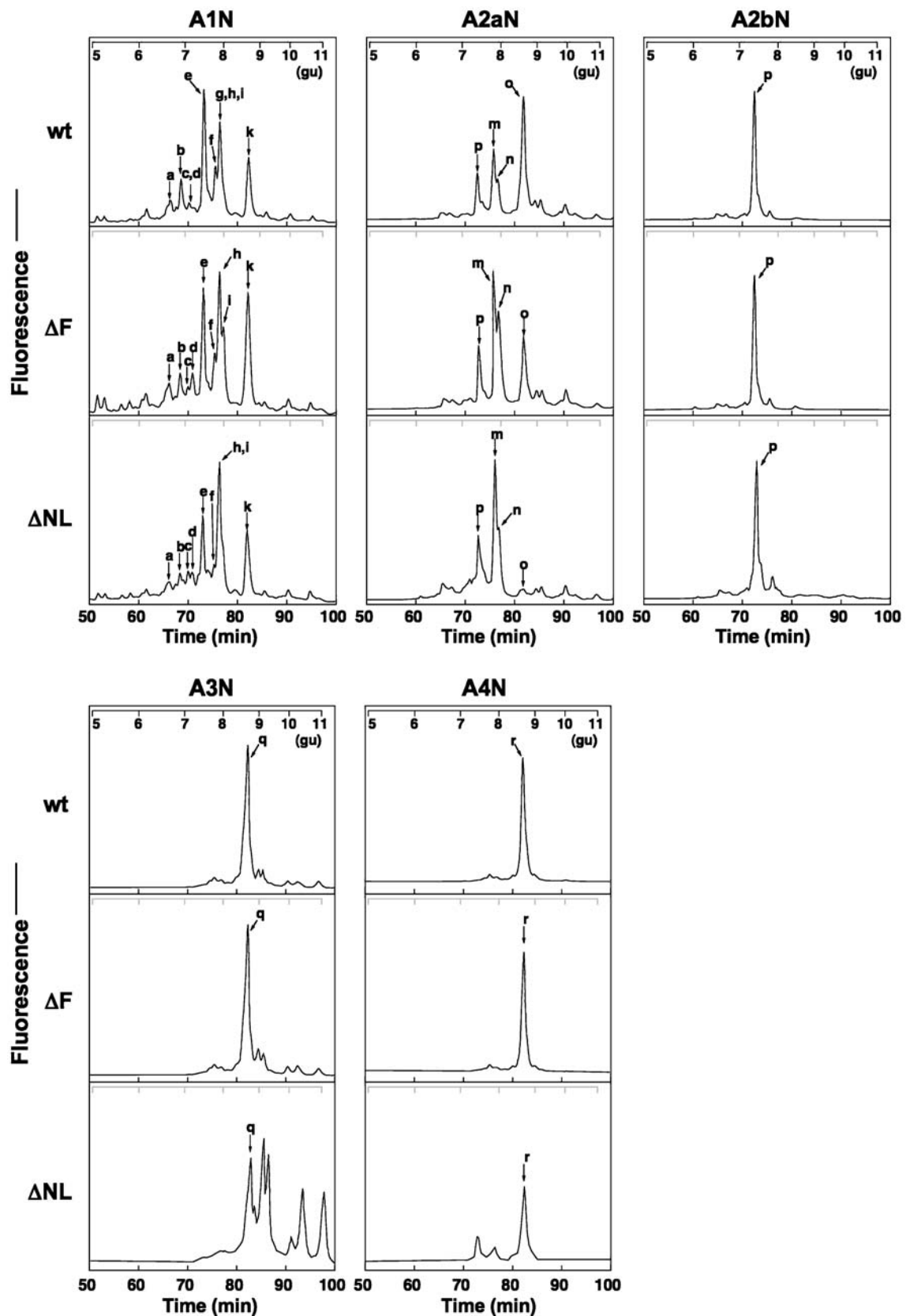
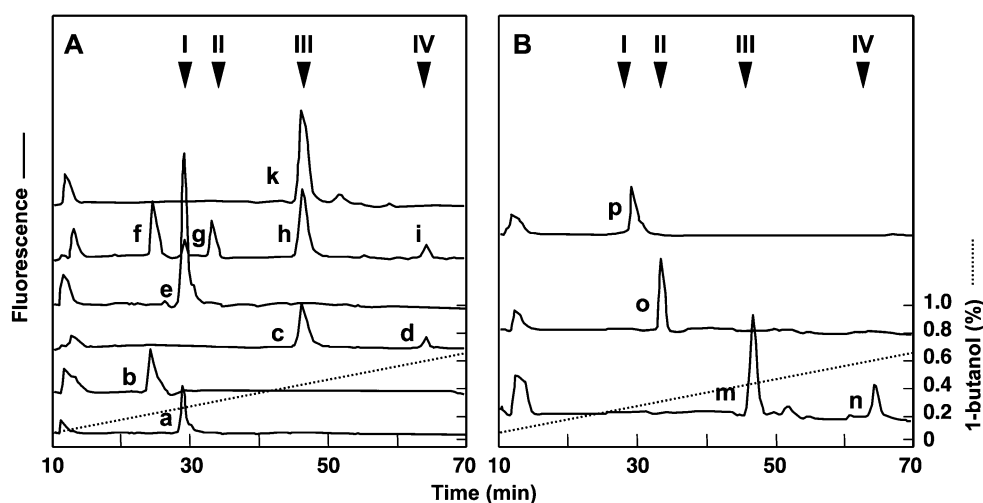


**Fig. 3** Normal phase column chromatography of the sialidase-digested components in each acidic fraction of *N*-glycans. After sialidase digestion of the A1, A2a, A2b, A3, and A4 fractions (Fig. 2), the A1N, A2aN, A2bN, A3N, and A4N fractions were recovered by Mono

Q column chromatography as neutral fractions. Each fraction was then applied to a GlycoSep N column, as described in the “[Experimental procedures](#).” Peaks were assigned GU values by comparison with the 2AB-labeled glucose oligomer ladder shown at the *top*

**Fig. 4** Reversed-phase column chromatography of components in A1N (a) and A2aN (b) fractions. Each component, which was fractionated by normal phase column chromatography (Fig. 3), was applied to a Cosmosil 5C<sub>18</sub>-AR column, as described in “Experimental procedures.” The closed triangles indicate the elution positions of the following 2AB-labeled authentic *N*-glycan standards: I, NA2; II, NA3; III, NA2F; IV, NA2FB



the same position as authentic NGA2 (B, 5.8 GU, Fig. 5a) with release of a galactose residue, and it was converted to a component with the same mobility as authentic M3 (S, 4.2 GU) by streptococcal  $\beta$ -*N*-acetylhexosaminidase, which cleaves the GlcNAc $\beta$ 1–2Man linkage only [20]. When component b was incubated sequentially with streptococcal  $\beta$ -galactosidase, streptococcal  $\beta$ -*N*-acetylhexosaminidase, and jack bean  $\alpha$ -mannosidase, it eluted at the same position as authentic M1 (M, 2.5 GU, Fig. 5b) with release of one galactose, one *N*-acetylglucosamine, and three mannose residues. When component c was incubated with streptococcal  $\beta$ -galactosidase, it eluted at the same position as authentic NGA2F (E, 6.2 GU, Fig. 5c) with release of a galactose residue; it was then converted to a component with the same mobility as authentic M3 (S, 4.2 GU) by sequential digestion with streptococcal  $\beta$ -*N*-acetylhexosaminidase and beef kidney  $\alpha$ -fucosidase. When component d was incubated with streptococcal  $\beta$ -galactosidase, it eluted at the same position as authentic NGA2FB (H, 6.5 GU, Fig. 5d) with release of a galactose residue; it was then converted to a component with the same mobility as authentic M3 (S, 4.2 GU) by sequential digestion with jack bean  $\beta$ -*N*-acetylhexosaminidase and beef kidney  $\alpha$ -fucosidase. Component e or p eluted at the same position as authentic NA2 (A, 7.2 GU, Fig. 5e,p) and was converted to a component with the same mobility as authentic M3 (S, 4.2 GU) with the release of two galactose and two *N*-acetylglucosamine residues by sequential digestion with streptococcal  $\beta$ -galactosidase and streptococcal  $\beta$ -*N*-acetylhexosaminidase, respectively. Component f was converted to a component with the same mobility as authentic M5 (N, 6.3 GU, Fig. 5f) with release of a galactose residue and an *N*-acetylglucosamine residue by sequential digestion with streptococcal  $\beta$ -galactosidase and streptococcal  $\beta$ -*N*-acetylhexosaminidase, respectively; four mannose residues were then removed by  $\alpha$ -mannosidase resulting in a fraction with the same mobility as authentic M1 (M, 2.5

GU, Fig. 5f). When component g was incubated with streptococcal  $\beta$ -galactosidase, it eluted at the same position as authentic NGA3 (L, 6.2 GU, Fig. 5g) with release of two galactose residues; it was then converted to a component with the same mobility as authentic M3 (S, 4.2 GU) by jack bean  $\beta$ -*N*-acetylhexosaminidase. Components h and m eluted at the same position as authentic NA2F (D, 7.8 GU, Fig. 5h, m) and were converted to a component with the same mobility as authentic M3 (S, 4.2 GU) with the release of two galactoses, two *N*-acetylglucosamines, and one fucose, respectively by sequential digestion with streptococcal  $\beta$ -galactosidase, streptococcal  $\beta$ -*N*-acetylhexosaminidase, and  $\alpha$ -fucosidase. Components i and n eluted at the same position as authentic NA2FB (G, 8.0 GU, Fig. 5i,n) and were converted into a component with the same mobility as authentic M3 (S, 4.2 GU) with the release of two galactoses, three *N*-acetylglucosamines, and one fucose, respectively, by sequential digestion with streptococcal  $\beta$ -galactosidase, jack bean  $\beta$ -*N*-acetylhexosaminidase, and  $\alpha$ -fucosidase. When component k was incubated with coffee bean  $\alpha$ -galactosidase, it eluted at the same position as authentic NGA2F (E, 6.2 GU, Fig. 5k) with release of a galactose residue, and was then converted into a component with the same mobility as authentic M3 (S, 4.2 GU) by sequential digestion with streptococcal  $\beta$ -galactosidase, streptococcal  $\beta$ -*N*-acetylhexosaminidase, and  $\alpha$ -fucosidase. In addition, when component k was incubated with endo  $\beta$ -galactosidase C, which cleaves the  $\beta$ -galactosidic linkage in the Gal $\alpha$ 1–3Gal $\beta$ 1–4GlcNAc sequence [18], two galactose residues were removed (Fig. 5k), indicating that the  $\alpha$ -galactosyl residue is linked to the 3-position of the  $\beta$ -galactose residue. Component o1 or q1 was eluted at the same position as authentic NA3 (K, 8.8 GU, Fig. 5o,q); they were converted into a component with the same mobility as authentic M3 (S, 4.2 GU) with the release of three galactose and three *N*-acetylglucosamine residues by streptococcal  $\beta$ -galactosidase and jack bean  $\beta$ -*N*-acetylhexosaminidase. Components o2, q2, and r eluted at the

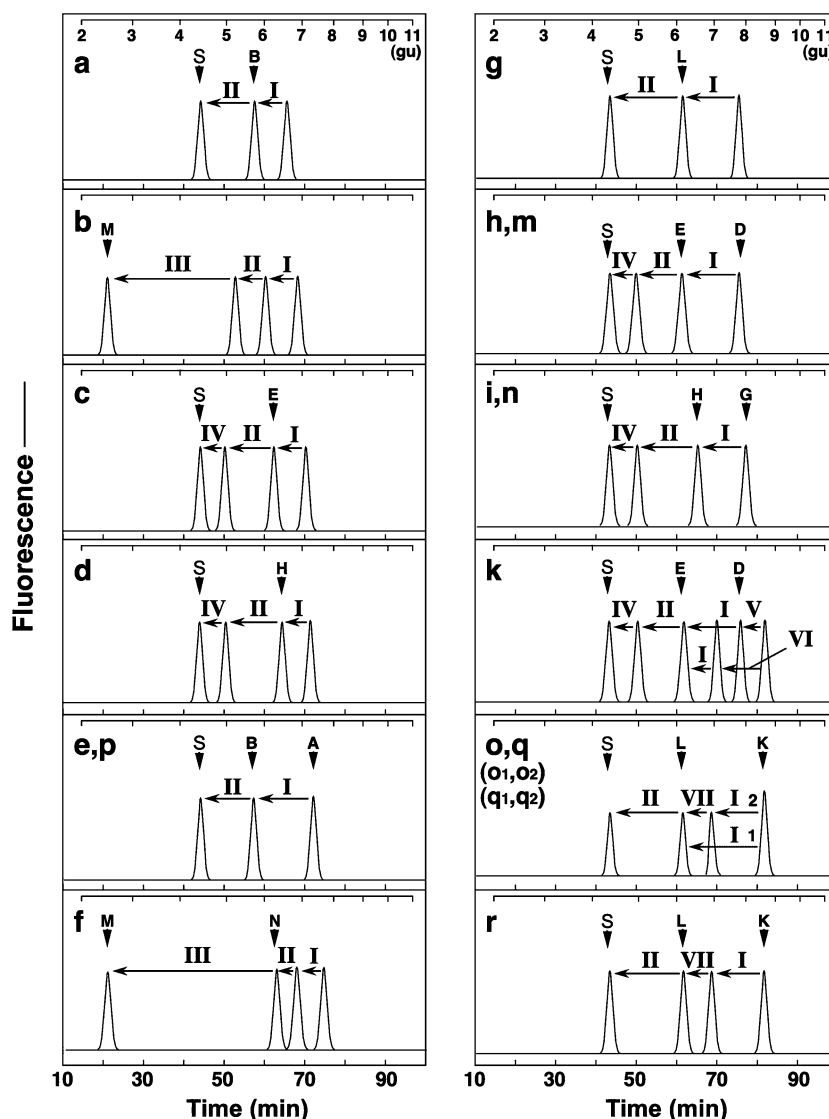


**Fig. 5** Sequential glycosidase digestion of each component in the acidic fraction. Each component (a–r) in Figs. 3 and 4 was fractionated as a single peak by reversed-phase and normal phase column chromatography. After digestion by a particular glycosidase, each component was then analyzed and recovered by reversed-phase and normal phase column chromatography. The displacements of the elution positions on normal phase column by sequential glycosidase digestion are shown. The arrows indicate displacements of elution position by digestion with the following glycosidases: I,  $\beta$ -galactosidase (*Streptococcus pneumoniae*); II,  $\beta$ -*N*-acetylhexosaminidase (jack

bean); III,  $\alpha$ -mannosidase (jack bean); IV,  $\alpha$ -fucosidase (beef kidney); V,  $\alpha$ -galactosidase (coffee bean); VI, endo- $\beta$ -galactosidase C (*Clostridium perfringens*); VII,  $\beta$ -galactosidase (*Streptococcus 6646K*). The arrowheads indicate the elution positions of the following 2AB-labeled authentic *N*-glycan standards: A, NA2; B, NGA2; D, NA2F; E, NGA2F; G, NG2FB; H, NGA2FB; K, NA3; L, NGA3; M, M1; N, M5; S, M3. Peaks were assigned GU values by comparison with the 2AB-labeled glucose oligomer ladder shown at the top. The structures and molar ratios of each component are summarized in Table 2

same position as authentic NA3 (K, 8.8 GU, Fig. 5o,q,r); however, when they were incubated with streptococcal  $\beta$ -galactosidase, only two galactose residues were removed. Nonetheless, when components o2, q2, and r were incubated with the  $\beta$ -galactosidase from *Streptococcus 6646K*, which cleaves both the Gal $\beta$ 1–3GlcNAc and Gal $\beta$ 1–4GlcNAc linkages, they eluted at the same position as authentic NGA3 (L, 6.2 GU, Fig. 5o,q,r).

The presence of bisecting *N*-acetylglucosamine residues and 2,4-branched triantennary glycans was determined

based on the substrate specificity of streptococcal  $\beta$ -*N*-acetylhexosaminidase. Thus, the non-galactosyl containing products of components d, i, and n released three *N*-acetylglucosamine residues by jack bean  $\beta$ -*N*-acetylhexosaminidase digestion, as described above. However, streptococcal  $\beta$ -*N*-acetylhexosaminidase digestion released only one *N*-acetylglucosamine residue (Fig. 6a and b). As reported previously [20], streptococcal  $\beta$ -*N*-acetylhexosaminidase cleaves only the GlcNAc $\beta$ 1–2Man linkage on the Man $\alpha$ 1–3 arm of *N*-glycans containing a bisecting *N*-

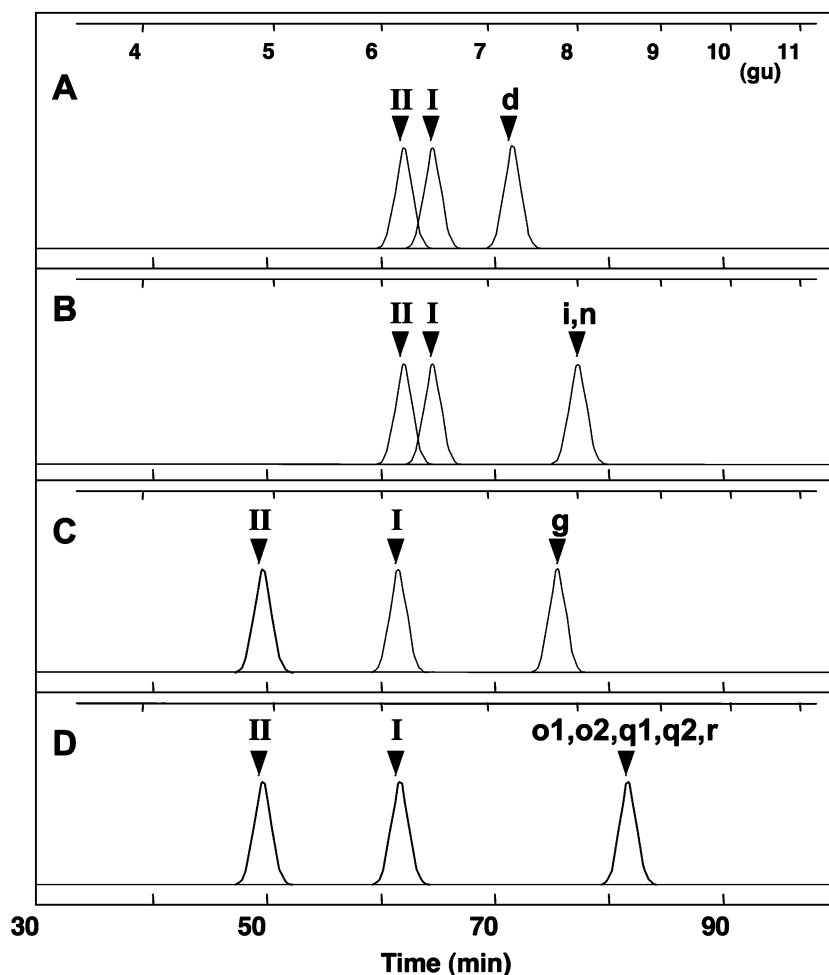


**Fig. 6** Identification of bisecting *N*-acetylglucosamine residues and 2,4-branched triantennary glycan structures. The presence of bisecting *N*-acetylglucosamine residues and 2,4-branched triantennary glycans were determined by digestion with streptococcal  $\beta$ -*N*-acetylhexosaminidase. **a** Component d; **b** components i and n; **c** component g; **d** components o1, o2, q1, q2, and r. After digestion by this glycosidase, each component was analyzed and recovered by reversed-phase and normal phase column chromatography. The displacements in the

elution positions by subsequent sequential glycosidase digestion were determined by normal phase column chromatography. Arrowheads indicate the elution positions after digestion with the following glycosidases: I,  $\beta$ -galactosidase (*Streptococcus 6646K*); II,  $\beta$ -*N*-acetylhexosaminidase (*Streptococcus pneumoniae*). Peaks were assigned GU values by comparison with the 2AB-labeled glucose oligomer ladder shown at the top

acetylglucosamine residue. In contrast, the non-galactosyl containing products of components g, o1, o2, q1, q2, and r released three *N*-acetylglucosamine residues when treated with jack bean  $\beta$ -*N*-acetylhexosaminidase, indicating that these are triantennary glycans. However, subsequent streptococcal  $\beta$ -*N*-acetylhexosaminidase digestion released only two *N*-acetylglucosamine residues (Fig. 6c and d). As reported previously [20], streptococcal  $\beta$ -*N*-acetylhexosaminidase only cleaves the GlcNAc $\beta$ 1–2Man linkage from the GlcNAc $\beta$ 1–2Man(GlcNAc $\beta$ 1–4Man) branch, but not from the GlcNAc $\beta$ 1–2Man(GlcNAc $\beta$ 1–6Man) branch, indicating that these were 2,4-branched, but not 2,6-branched, *N*-glycans. Taken together, the structures and molar ratios of each component from the *N*-glycan acidic fractions are summarized in Table 2.

As shown in Table 2, the three different APPs contained predominantly bi-antennary complex type *N*-glycans. Interestingly, in comparison with wild-type APP, both mutant APPs had higher contents of *N*-glycans containing bisecting *N*-acetylglucosamine and core-fucose residues (components c, d, h, i, k, m, and n). The total contents of *N*-glycans having bisecting *N*-acetylglucosamine and/or core-fucose residues from each APP are summarized in Table 3. The percentages of *N*-glycans with bisecting *N*-acetylglucosamines isolated from wild-type,  $\Delta$ F, and  $\Delta$ NL APP were 1.7%, 13.2%, and 15.0%, respectively. Similarly, the core-fucose contents of the *N*-glycans of wild-type,  $\Delta$ F, and  $\Delta$ NL APP were 15.1%, 34.4%, and 49.8%, respectively. Thus, the bisecting *N*-acetylglucosamine and core-fucose type *N*-glycans of these mutant APPs were approximately

**Table 2** Structures and molar ratios of the *N*-glycans in the acidic fractions of wild-type and mutant APP

component	structure	molar ratio (%)			component	structure	molar ratio (%)		
		wt	ΔF	ΔNL			wt	ΔF	ΔNL
<b>A1N</b>									
a	↑Galβ1→4GlcNAcβ1→2Manα1→6Manβ1→4GlcNAcβ1→4GlcNAc—2AB	2.1	3.1	2.6	m	Galβ1→4GlcNAcβ1→2Manα1→6Manβ1→4GlcNAcβ1→4GlcNAc—2AB	2.9	6.0	16.7
	↓Galβ1→4GlcNAcβ1→2Manα1→3Manβ1→4GlcNAcβ1→4GlcNAc—2AB								
b	Manα1→XManα1→6Manβ1→4GlcNAcβ1→4GlcNAc—2AB Galβ1→4GlcNAcβ1→2Manα1→3Manβ1→4GlcNAcβ1→4GlcNAc—2AB	2.6	3.1	3.1	n	Galβ1→4GlcNAcβ1→2Manα1→6Manβ1→4GlcNAcβ1→4GlcNAc—2AB Galβ1→4GlcNAcβ1→2Manα1→3Manβ1→4GlcNAcβ1→4GlcNAc—2AB	1.7	6.4	10.9
c	↑Galβ1→4GlcNAcβ1→2Manα1→6Manβ1→4GlcNAcβ1→4GlcNAc—2AB	1.1	1.2	1.6	o1	Galβ1→4GlcNAcβ1→2Manα1→6Manβ1→4GlcNAcβ1→4GlcNAc—2AB	5.4	4.7	2.3
	↓Galβ1→4GlcNAcβ1→2Manα1→3Manβ1→4GlcNAcβ1→4GlcNAc—2AB								
d	↑Galβ1→4GlcNAcβ1→2Manα1→6Manβ1→4GlcNAcβ1→4GlcNAc—2AB	tr.*	3.1	2.2	o2	Galβ1→4GlcNAcβ1→2Manα1→6Manβ1→4GlcNAcβ1→4GlcNAc—2AB	1.0	1.1	tr.*
	↓Galβ1→4GlcNAcβ1→2Manα1→3Manβ1→4GlcNAcβ1→4GlcNAc—2AB								
e	Galβ1→4GlcNAcβ1→2Manα1→6Manβ1→4GlcNAcβ1→4GlcNAc—2AB Galβ1→4GlcNAcβ1→2Manα1→3Manβ1→4GlcNAcβ1→4GlcNAc—2AB	7.1	7.6	5.8	p	Galβ1→4GlcNAcβ1→2Manα1→6Manβ1→4GlcNAcβ1→4GlcNAc—2AB Galβ1→4GlcNAcβ1→2Manα1→3Manβ1→4GlcNAcβ1→4GlcNAc—2AB	45.7	33.9	30.4
f	Manα1→6Manα1→6Manβ1→4GlcNAcβ1→4GlcNAc—2AB Galβ1→4GlcNAcβ1→2Manα1→3Manβ1→4GlcNAcβ1→4GlcNAc—2AB	2.6	2.4	2.0	<b>A3N</b>				
g	↑Galβ1→4GlcNAcβ1→2Manα1→6Manβ1→4GlcNAcβ1→4GlcNAc—2AB	1.1	.**	.**	q1	Galβ1→4GlcNAcβ1→2Manα1→6Manβ1→4GlcNAcβ1→4GlcNAc—2AB	7.0	4.7	tr.*
	↓Galβ1→4GlcNAcβ1→2Manα1→3Manβ1→4GlcNAcβ1→4GlcNAc—2AB								
h	↑Galβ1→4GlcNAcβ1→2Manα1→6Manβ1→4GlcNAcβ1→4GlcNAc—2AB	3.9	5.6	10.0	q2	Galβ1→4GlcNAcβ1→2Manα1→6Manβ1→4GlcNAcβ1→4GlcNAc—2AB	3.5	1.7	tr.*
	↓Galβ1→4GlcNAcβ1→2Manα1→3Manβ1→4GlcNAcβ1→4GlcNAc—2AB								
i	↑Galβ1→4GlcNAcβ1→2Manα1→6Manβ1→4GlcNAcβ1→4GlcNAc—2AB	tr.*	3.7	1.9	<b>A4N</b>				
	↓Galβ1→4GlcNAcβ1→2Manα1→3Manβ1→4GlcNAcβ1→4GlcNAc—2AB								
k	↑Galα1→3Galβ1→4GlcNAcβ1→2Manα1→6Manβ1→4GlcNAcβ1→4GlcNAc—2AB	4.4	8.4	6.5	r	Galβ1→4GlcNAcβ1→2Manα1→6Manβ1→4GlcNAcβ1→4GlcNAc—2AB	6.6	3.3	2.1
	↓Galα1→3Galβ1→4GlcNAcβ1→2Manα1→3Manβ1→4GlcNAcβ1→4GlcNAc—2AB								

eight to nine times and approximately two to three times greater than those of wild-type APP, respectively. In contrast, the content of tri-antennary complex type *N*-glycans (*i.e.* components g, o1, o2, q1, q2, and r; see Table 2) from both mutants were each less than those from wild-type APP. Taken together, these results suggest that a change in acidic *N*-glycan processing occurs on APPs carrying these particular familial AD mutations.

**Structural Study of *N*-glycans from Neutral Fractions** The structures of the *N*-glycans from the neutral fractions isolated by Mono Q chromatography (Fig. 2) were analyzed by the same methods used for acidic fractions described above. As shown in Fig. 7a, the neutral *N*-glycans from each APP had a similar elution profile on normal phase column chromatography. The N1 and N2 components eluted at the same position as authentic NGA2F (6.2 GU) and M5 (6.3 GU), respectively. Only component N2 could be digested by α-mannosidase (Fig. 7b; and co-migrated with authentic M1, not shown in the figure). Several components in the N3 fraction were converted into components N4 and N5, with the same mobility as authentic NGA2 (5.8 GU, N4) and NGA2FB (6.5 GU, N5), by digestion with streptococcal β-galactosidase (Fig. 7c). Components N6 and N7 eluted at the same position as authentic M3 and M3F, respectively, and were derived from component N1 and several components in the N3 fraction by digestion with streptococcal β-galactosidase

and jack bean β-*N*-acetylhexosaminidase (Fig. 7d). In contrast, component N2 was not digested by either streptococcal β-galactosidase or jack bean β-*N*-acetylhexosaminidase (Fig. 7d). Based on these results, the structures of the *N*-glycans in the neutral fractions are summarized in Table 4.

**Discussion**

We are interested in whether APP *N*-glycans play a role in the pathobiology of AD. To determine whether mutations in the *APP* gene alter the structures of the *N*-glycans attached to the APP polypeptide, we expressed wild-type (*i.e.* wt) and two mutant APPs (*i.e.* ΔF and ΔNL) in transfected mouse neuroblastoma C17 cells. We previously reported

**Table 3** Characteristics of the *N*-glycans of wild type and mutant APPs

	Types of <i>N</i> -glycans (% molar ratio)	
	Core-fucose	Bisecting GlcNAc
wt	15.5	1.7
ΔF	34.4	13.2
ΔNL	49.8	15.0

**Table 4** Neutral *N*-glycan structures from each APP

component	structure
N1	$\begin{array}{c} \text{GlcNAc}\beta 1 \rightarrow 2\text{Man}\alpha 1 \begin{array}{l} \searrow 6 \\ \nearrow 3 \end{array} \\ \text{GlcNAc}\beta 1 \rightarrow 2\text{Man}\alpha 1 \end{array} \text{Man}\beta 1 \rightarrow 4\text{GlcNAc}\beta 1 \rightarrow 4\text{GlcNAc} \text{---} 2\text{AB}$ $\text{Fuc}\alpha 1 \downarrow 6$
N2	$\begin{array}{c} \text{Man}\alpha 1 \begin{array}{l} \searrow 6 \\ \nearrow 3 \end{array} \\ \text{Man}\alpha 1 \end{array} \text{Man}\alpha 1 \begin{array}{l} \searrow 6 \\ \nearrow 3 \end{array} \\ \text{Man}\alpha 1 \end{array} \text{Man}\beta 1 \rightarrow 4\text{GlcNAc}\beta 1 \rightarrow 4\text{GlcNAc} \text{---} 2\text{AB}$
N3	$\begin{array}{c} (\text{Gal}\beta 1 \rightarrow 4)_{1-2} \left( \begin{array}{c} \text{GlcNAc}\beta 1 \rightarrow 2\text{Man}\alpha 1 \begin{array}{l} \searrow 6 \\ \nearrow 3 \end{array} \\ \text{GlcNAc}\beta 1 \rightarrow 2\text{Man}\alpha 1 \end{array} \right) \text{Man}\beta 1 \rightarrow 4\text{GlcNAc}\beta 1 \rightarrow 4\text{GlcNAc} \text{---} 2\text{AB}$ $\text{Fuc}\alpha 1 \downarrow 6$ $\begin{array}{c} (\text{Gal}\beta 1 \rightarrow 4)_{1-2} \left( \begin{array}{c} \text{GlcNAc}\beta 1 \rightarrow 2\text{Man}\alpha 1 \begin{array}{l} \searrow 6 \\ \nearrow 3 \end{array} \\ \text{GlcNAc}\beta 1 \rightarrow 2\text{Man}\alpha 1 \end{array} \right) \text{Man}\beta 1 \rightarrow 4\text{GlcNAc}\beta 1 \rightarrow 4\text{GlcNAc} \text{---} 2\text{AB}$ $\text{Fuc}\alpha 1 \downarrow 6$ $\begin{array}{c} (\text{Gal}\beta 1 \rightarrow 4)_{1-2} \left( \begin{array}{c} \text{GlcNAc}\beta 1 \rightarrow 2\text{Man}\alpha 1 \begin{array}{l} \searrow 6 \\ \nearrow 3 \end{array} \\ \text{GlcNAc}\beta 1 \rightarrow 2\text{Man}\alpha 1 \end{array} \right) \text{Man}\beta 1 \rightarrow 4\text{GlcNAc}\beta 1 \rightarrow 4\text{GlcNAc} \text{---} 2\text{AB}$ $\text{Fuc}\alpha 1 \downarrow 6$
N4	$\begin{array}{c} \text{GlcNAc}\beta 1 \rightarrow 2\text{Man}\alpha 1 \begin{array}{l} \searrow 6 \\ \nearrow 3 \end{array} \\ \text{GlcNAc}\beta 1 \rightarrow 2\text{Man}\alpha 1 \end{array} \text{Man}\beta 1 \rightarrow 4\text{GlcNAc}\beta 1 \rightarrow 4\text{GlcNAc} \text{---} 2\text{AB}$
N5	$\begin{array}{c} \text{GlcNAc}\beta 1 \rightarrow 2\text{Man}\alpha 1 \begin{array}{l} \searrow 6 \\ \nearrow 3 \end{array} \\ \text{GlcNAc}\beta 1 \rightarrow 2\text{Man}\alpha 1 \end{array} \text{Man}\beta 1 \rightarrow 4\text{GlcNAc}\beta 1 \rightarrow 4\text{GlcNAc} \text{---} 2\text{AB}$ $\text{Fuc}\alpha 1 \downarrow 6$
N6	$\begin{array}{c} \text{Man}\alpha 1 \begin{array}{l} \searrow 6 \\ \nearrow 3 \end{array} \\ \text{Man}\alpha 1 \end{array} \text{Man}\beta 1 \rightarrow 4\text{GlcNAc}\beta 1 \rightarrow 4\text{GlcNAc} \text{---} 2\text{AB}$
N7	$\begin{array}{c} \text{Man}\alpha 1 \begin{array}{l} \searrow 6 \\ \nearrow 3 \end{array} \\ \text{Man}\alpha 1 \end{array} \text{Man}\beta 1 \rightarrow 4\text{GlcNAc}\beta 1 \rightarrow 4\text{GlcNAc} \text{---} 2\text{AB}$ $\text{Fuc}\alpha 1 \downarrow 6$

the *N*-glycan structures of APP695 produced by Chinese hamster ovary cells [12]; this recombinant APP695 has sialylated bi- and triantennary complex type *N*-glycans with fucosylated and non-fucosylated trimannosyl cores. As reported here, we found similar *N*-glycan structures on wild-type APP produced by C17 cells except for the presence of *N*-glycans containing bisecting *N*-acetylglucosamine. This finding is not surprising, because it is well known that cell type-specific differences in *N*-glycans can be found with recombinant glycoproteins [21, 22]. However, structural analysis of the *N*-glycans revealed that the two mutant APPs had high contents of bisecting *N*-acetylglucosamine and core-fucose residues as compared to wild-type APP (Table 3). The two mutant APPs had this feature in common, although they had different amino acid mutations. The differences in APP *N*-glycan processing must be induced by effects derived from the different

primary amino acid sequences of the recombinant forms of APP, because each transfected C17 cell line has the same set of glycosylation machinery encoded by the host cell. For example, changing the amino acid sequence of APP may affect its rate of transport through the secretory apparatus or influence the interactions of the nascent glycoprotein with the relevant glycosyltransferases. The *N*-glycan alterations of the mutant APPs may also affect production of A $\beta$  by the relevant secretases.

The addition of a bisecting *N*-acetylglucosamine or a core-fucose is an important modification of *N*-glycans. The glycosyltransferases responsible for forming bisecting *N*-acetylglucosamine and core-fucose structures are GnT-III and FUT8, respectively [23–26]. The addition of a bisecting *N*-acetylglucosamine to *N*-glycans is regulated during development and has functional consequences for receptor signaling, cell adhesion, and tumor progression [27]. For

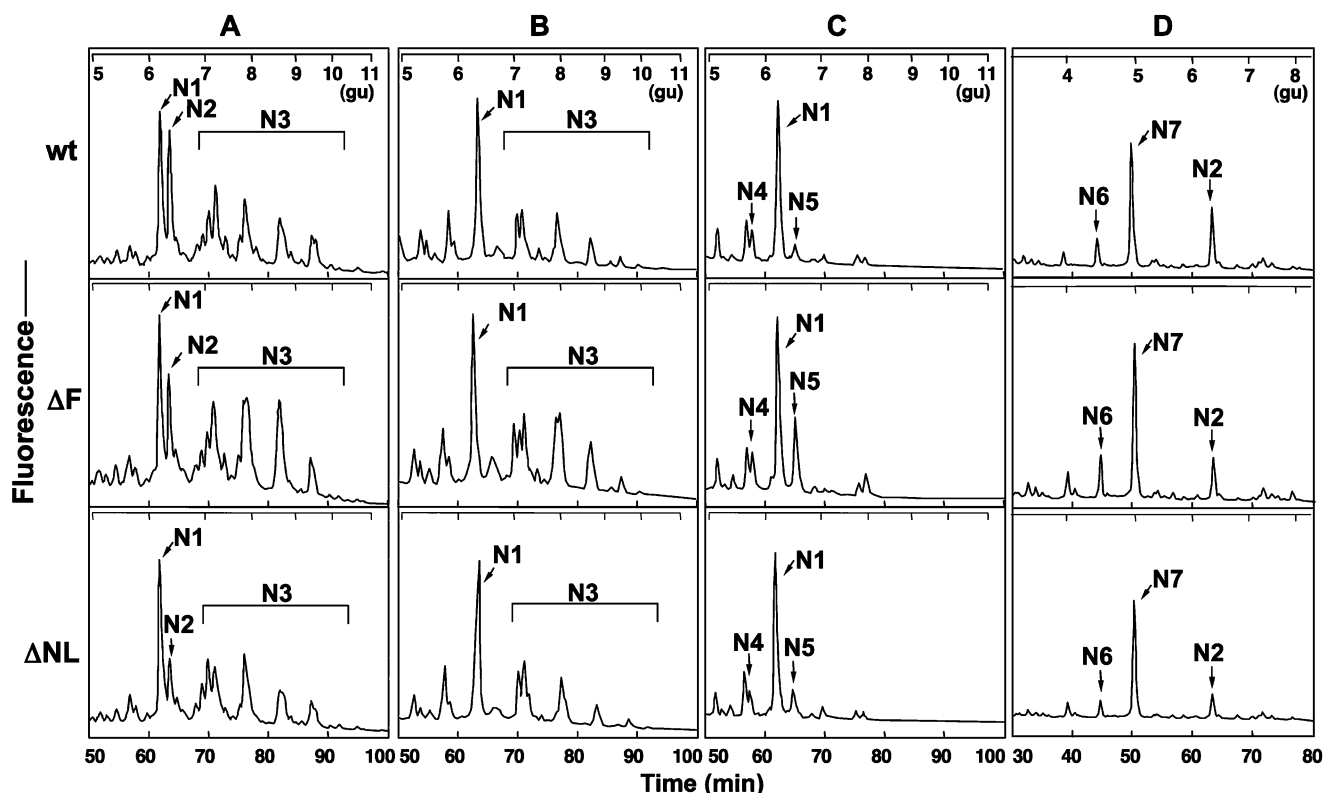


**Fig. 7** Structural study of the recombinant APP neutral *N*-glycans. The *N* fractions from Mono Q column chromatography (Fig. 2) were analyzed with GlycoSep *N* column chromatography and sequential glycosidase digestion. **a** *N* fractions; **b**  $\alpha$ -mannosidase digestion products of *N* fractions; **c**  $\alpha$ -mannosidase and streptococcal  $\beta$ -

galactosidase digestion products of *N* fractions; **d** streptococcal  $\beta$ -galactosidase and jack bean  $\beta$ -*N*-acetylhexosaminidase digestion products of *N* fractions. Peaks were assigned GU values by comparison with the 2AB-labeled glucose oligomer ladder shown at the top. The structure of each component is summarized in Table 4

example, in prion disease there are glycosylation differences between normal (PrP<sup>C</sup>) and pathogenic (PrP<sup>Sc</sup>) prion protein isoforms [28]. Thus, compared with PrP<sup>C</sup>, PrP<sup>Sc</sup> contains decreased levels of *N*-glycans with bisecting *N*-acetylglucosamine residues and increased levels of tri- and tetraantennary *N*-glycans. This may be due to the decrease in the activity of GnT-III in the prion disease process. As another example, expression of a truncated, inactive GnT-III protein in murine brain leads to neurological dysfunction [29]. These studies suggest that a decrease in bisecting *N*-acetylglucosamine residues on the *N*-glycans of brain glycoproteins results in neurological dysfunction. This may also relate to a previous finding that expression of GnT-III potentiates neurogenesis [30]. Taken together, bisecting *N*-glycans on brain glycoproteins may play a significant role in normal and pathological neurological function.

The functional roles of core-fucosylation of *N*-glycans on brain glycoproteins are poorly understood; however, several important findings in other systems were reported recently. For example, core-fucosylation of IgG *N*-glycans regulates antibody-dependent cellular cytotoxicity [31, 32]. In addition, core-fucosylation of the *N*-glycans of epidermal growth factor, integrins, and transforming growth factor- $\beta$

are required for appropriate signal transduction [30, 33, 34]. Finally, *FUT8* gene deficiency in mice leads to growth retardation, emphysema, and death during early post-natal development [35]. These findings suggested that the core-fucose residue is important in various physiological and pathological situations [27].

In this study, we demonstrated an increase in the presence of bisecting *N*-acetylglucosamine and core-fucose structures of the *N*-glycans on the mutant APPs found in early-onset familial AD. Alteration of the *N*-glycans may cause conformational changes of the APP glycoprotein, thereby altering its susceptibility to cleavage by the  $\beta$ - and  $\gamma$ -secretases. Thus, it is possible that alteration of the APP *N*-glycans influences A $\beta$  production and may be relevant to the high production of A $\beta$  in these types of familial AD. In addition, changes of *N*-glycan structure may affect the normal, physiological function of APP in neuronal cells. Nonetheless, these latter hypotheses remain to be tested.

**Acknowledgement** We would like to thank Dr. Takashi Muramatsu for providing an endo- $\beta$ -galactosidase C. This study was supported by a Grant-in-Aid for Scientific Research (20390031) from the Japan Society for the Promotion of Science.

## References

- Price, D.L., Sisodia, S.S., Borchelt, D.R.: *Science* **282**, 1079–1083 (1998)
- Sinha, S., Lieberburg, I.: *Proc. Natl. Acad. Sci. U.S.A.* **96**, 11049–11053 (1999)
- Rutishauser, U., Landmesser, L.: *Trends Neurosci.* **19**, 422–427 (1996)
- Seki, T., Arai, Y.: *Neuroreport* **6**, 2479–2482 (1995)
- Sato, Y., Endo, T.: *Neurosci. Lett.* **262**, 49–52 (1999)
- Taketa, K., Endo, Y., Sekiya, C., Tanikawa, K., Koji, T., Taga, H., Satomura, S., Matsuura, S., Kawai, T., Hirai, H.: *Cancer Res.* **53**, 5419–5423 (1993)
- Sato, Y., Nakata, K., Kato, Y., Shima, M., Ishii, N., Koji, T., Taketa, K., Endo, Y., Nagataki, S.: *N. Engl. J. Med.* **328**, 1802–1806 (1993)
- Miyazaki, K., Ohmori, K., Izawa, M., Koike, T., Kumamoto, K., Furukawa, K., Ando, T., Kiso, M., Yamaji, T., Hashimoto, Y., Suzuki, A., Yoshida, A., Takeuchi, M., Kannagi, R.: *Cancer Res.* **64**, 4498–4505 (2004)
- Ohtsubo, K., Marth, J.D.: *Cell* **126**, 855–867 (2006)
- Weidemann, A., Konig, G., Bunke, D., Fischer, P., Salbaum, J.M., Masters, C.L., Beyreuther, K.: *Cell* **57**, 115–126 (1989)
- Tomita, S., Kirino, Y., Suzuki, T.: *J. Biol. Chem.* **273**, 6277–6284 (1998)
- Sato, Y., Liu, C., Wojczyk, B.S., Kobata, A., Spitalnik, S.L., Endo, T.: *Biochim. Biophys. Acta* **1472**, 344–358 (1999)
- Yazaki, M., Tagawa, K., Maruyama, K., Sorimachi, H., Tsuchiya, T., Ishiura, S., Suzuki, K.: *Neurosci. Lett.* **221**, 57–60 (1996)
- Pahlsson, P., Shakin-Eshleman, S.H., Spitalnik, S.L.: *Biochem. Biophys. Res. Commun.* **189**, 1667–1673 (1992)
- Saito, F., Tani, A., Miyatake, T., Yanagisawa, K.: *Biochem. Biophys. Res. Commun.* **210**, 703–710 (1995)
- Citron, M., Oltersdorf, T., Haass, C., McConlogue, L., Hung, A. Y., Seubert, P., Vigo-Pelfrey, C., Lieberburg, I., Selkoe, D.J.: *Nature* **360**, 672–674 (1992)
- Suzuki, N., Cheung, T.T., Cai, X.D., Odaka, A., Otvos, Jr. L., Eckman, C., Golde, T.E., Younkin, S.G.: *Science* **264**, 1336–1340 (1994)
- Ogawa, H., Muramatsu, H., Kobayashi, T., Morozumi, K., Yokoyama, I., Kurosawa, N., Nakao, A., Muramatsu, T.: *J. Biol. Chem.* **275**, 19368–19374 (2000)
- Manya, H., Sato, Y., Eguchi, N., Seiki, K., Oda, H., Nakajima, H., Urade, Y., Endo, T.: *J. Biochem. (Tokyo)* **127**, 1001–1011 (2000)
- Yamashita, K., Ohkura, T., Yoshima, H., Kobata, A.: *Biochem. Biophys. Res. Commun.* **100**, 226–232 (1981)
- Cumming, D.A.: *Glycobiology* **1**, 115–130 (1991)
- Kagawa, Y., Takasaki, S., Utsumi, J., Hosoi, K., Shimizu, H., Kochibe, N., Kobata, A.: *J. Biol. Chem.* **263**, 17508–17515 (1988)
- Nishikawa, A., Ihara, Y., Hatakeyama, M., Kangawa, K., Taniguchi, N.: *J. Biol. Chem.* **267**, 18199–18204 (1992)
- Narasimhan, S.: *J. Biol. Chem.* **257**, 10235–10242 (1982)
- Wilson, J.R., Williams, D., Schachter, H.: *Biochem. Biophys. Res. Commun.* **72**, 909–916 (1976)
- Uozumi, N., Yanagidani, S., Miyoshi, E., Ihara, Y., Sakuma, T., Gao, C.X., Teshima, T., Fujii, S., Shiba, T., Taniguchi, N.: *J. Biol. Chem.* **271**, 27810–27817 (1996)
- Kondo, A., Li, W., Nakagawa, T., Nakano, M., Koyama, N., Wang, X., Gu, J., Miyoshi, E., Taniguchi, N.: *Biochim. Biophys. Acta* **1764**, 1881–1889 (2006)
- Rudd, P.M., Endo, T., Colominas, C., Groth, D., Wheeler, S.F., Harvey, D.J., Wormald, M.R., Serban, H., Prusiner, S.B., Kobata, A., Dwek, R.A.: *Proc. Natl. Acad. Sci. U.S.A.* **96**, 13044–13049 (1999)
- Bhattacharyya, R., Bhaumik, M., Raju, T.S., Stanley, P.: *J. Biol. Chem.* **277**, 26300–26309 (2002)
- Shigeta, M., Shibukawa, Y., Ihara, H., Miyoshi, E., Taniguchi, N., Gu, J.: *Glycobiology* **16**, 564–571 (2006)
- Shields, R.L., Lai, J., Keck, R., O'Connell, L.Y., Hong, K., Meng, Y.G., Weikert, S.H., Presta, L.G.: *J. Biol. Chem.* **277**, 26733–26740 (2002)
- Shinkawa, T., Nakamura, K., Yamane, N., Shoji-Hosaka, E., Kanda, Y., Sakurada, M., Uchida, K., Anazawa, H., Satoh, M., Yamasaki, M., Hanai, N., Shitara, K.: *J. Biol. Chem.* **278**, 3466–3473 (2003)
- Wang, X., Gu, J., Ihara, H., Miyoshi, E., Honke, K., Taniguchi, N.: *J. Biol. Chem.* **281**, 2572–2577 (2006)
- Zhao, Y., Itoh, S., Wang, X., Isaji, T., Miyoshi, E., Kariya, Y., Miyazaki, K., Kawasaki, N., Taniguchi, N., Gu, J.: *J. Biol. Chem.* **281**, 38343–38350 (2006)
- Wang, X., Inoue, S., Gu, J., Miyoshi, E., Noda, K., Li, W., Mizuno-Horikawa, Y., Nakano, M., Asahi, M., Takahashi, M., Uozumi, N., Ihara, S., Lee, S.H., Ikeda, Y., Yamaguchi, Y., Aze, Y., Tomiyama, Y., Fujii, J., Suzuki, K., Kondo, A., Shapiro, S.D., Lopez-Otin, C., Kuwaki, T., Okabe, M., Honke, K., Taniguchi, N.: *Proc. Natl. Acad. Sci. U.S.A.* **102**, 15791–15796 (2005)